Author Manuscript Published OnlineFirst on February 26, 2019; DOI: 10.1158/1541-7786.MCR-18-1147
Author manuscripts have been peer reviewed and accepted for publication but have not yet been edited.

Lipid uptake is an androgen-enhanced lipid supply pathway associated with prostate cancer disease progression and bone metastasis

Kaylyn D Tousignant[1], Anja Rockstroh[1], Atefeh Taherian Fard[1], Melanie L Lehman[1], Chenwei Wang[1], Stephen J McPherson[1], Lisa K Philp[1], Nenad Bartonicek[2,3], Marcel E Dinger[2,3], Colleen C Nelson[1], Martin C Sadowski[1]

[1]Australian Prostate Cancer Research Centre - Queensland, Institute of Health and Biomedical Innovation, School of Biomedical Sciences, Faculty of Health, Queensland University of Technology, Princess Alexandra Hospital, Translational Research Institute

[2] Kinghorn Centre for Clinical Genomics, Garvan Institute of Medical Research, Sydney, Australia

[3] St Vincent's Clinical School, UNSW Sydney, Sydney, Australia

Keywords: lipid uptake, androgen signaling, low-density lipoprotein receptor (LDLR), scavenger receptor class B type 1 (SCARB1), prostate cancer

Disclosure of Potential Conflicts of Interest

No potential conflicts of interest were disclosed.

Author Manuscript Published OnlineFirst on February 26, 2019; DOI: 10.1158/1541-7786.MCR-18-1147
Author manuscripts have been peer reviewed and accepted for publication but have not yet been edited.

Abstract

De novo lipogenesis is a well-described AR-regulated metabolic pathway that supports prostate cancer tumor growth by providing fuel, membrane material and steroid hormone precursor. In contrast, our current understanding of lipid supply from uptake of exogenous lipids and its regulation by AR is limited, and exogenous lipids may play a much more significant role in prostate cancer and disease progression than previously thought. By applying advanced automated quantitative fluorescence microscopy, we provide the most comprehensive functional analysis of lipid uptake in cancer cells to date and demonstrate that treatment of AR-positive prostate cancer cell lines with androgens results in significantly increased cellular uptake of fatty acids, cholesterol and low density lipoprotein particles. Consistent with a direct, regulatory role of AR in this process, androgen-enhanced lipid uptake can be blocked by AR-antagonist Enzalutamide, but is independent of proliferation and cell cycle progression. This work for the first time comprehensively delineates the lipid transporter landscape in prostate cancer cell lines and patient samples by analysis of transcriptomics and proteomics data, including the plasma membrane proteome. We show that androgen exposure or deprivation regulates the expression of multiple lipid transporters in prostate cancer cell lines and tumor xenografts and that mRNA and protein expression of lipid transporters is enhanced in bone metastatic disease when compared to primary, localized prostate cancer. Our findings provide a strong rationale to investigate lipid uptake as a therapeutic co-target in the fight against advanced prostate cancer in combination with inhibitors of lipogenesis to delay disease progression and metastasis.

Author Manuscript Published OnlineFirst on February 26, 2019; DOI: 10.1158/1541-7786.MCR-18-1147
Author manuscripts have been peer reviewed and accepted for publication but have not yet been edited.

Implications

Prostate cancer exhibits metabolic plasticity in acquiring lipids from uptake and lipogenesis at different disease stages, indicating potential therapeutic benefit by co-targeting lipid supply.

Author Manuscript Published OnlineFirst on February 26, 2019; DOI: 10.1158/1541-7786.MCR-18-1147
Author manuscripts have been peer reviewed and accepted for publication but have not yet been edited.

Introduction

The role of lipid metabolism in the incidence and progression of prostate cancer and several other cancer types has gained notable attention in an attempt to develop new therapeutic interventions. Lipids represent a diverse group of compounds derived from fatty acids and cholesterol that serve an essential role in many physiological and biochemical processes. They function in energy generation and storage as well as intracellular signaling, protein modification, and precursor for steroid hormone synthesis. Additionally, fatty acids serve as the main building blocks for phospholipids that are incorporated together with free cholesterol into membranes and are critical for membrane function, cell signaling and proliferation.

As a source of lipid supply, uptake of circulating exogenous lipids is sufficient for the requirements of most normal cells, and following development, lipogenic enzymes remain expressed at relatively low levels apart from a few specific biological processes (surfactant production in the lungs, production of fatty acids for milk lipids during lactation, and steroidogenic activity in tissues including prostate). However, lipogenic pathways, i.e. *de novo* lipogenesis (DNL) of fatty acids and cholesterol, are reactivated or upregulated in many solid cancer types, including prostate cancer. Enhanced lipogenesis is now acknowledged as a metabolic hallmark of cancer and is an early metabolic switch in the development of prostate cancer. It is maintained throughout the progression of prostate cancer and associated with poor prognosis and aggressiveness of disease. [1-5]. Yet, the contribution and identity of lipid uptake pathways as a supply route of exogenous lipids and their role in disease development and progression remain largely unknown.

Several lipogenic enzymes, including fatty acid synthase (FASN), are found to be overexpressed in prostate cancer [reviewed in [1]]. Because increased *FASN* gene copy number, transcriptional activation or protein expression are common characteristics of

Author Manuscript Published OnlineFirst on February 26, 2019; DOI: 10.1158/1541-7786.MCR-18-1147
Author manuscripts have been peer reviewed and accepted for publication but have not yet been edited.

prostate cancer, fatty acid and cholesterol synthesis have become an attractive therapeutic target. However the antineoplastic effects observed by inhibiting lipogenesis can be rescued by the addition of exogenous lipids [6, 7], highlighting lipid uptake as a mechanism of clinical resistance to lipogenesis inhibitors and that lipid uptake capacity is sufficient to substitute for the loss of lipogenesis. Indeed, it was recently reported that lung cancer cells expressing a strong lipogenic phenotype generated up to 70% of their cellular lipid carbon biomass from exogenous fatty acids and only 30% from *de novo* synthesis supplied by glucose and glutamine as carbon sources [8]. While altered cellular lipid metabolism is a hallmark of the malignant phenotype, prostate cancer is unique in that it is characterized by a relatively low uptake of glucose and glycolytic rate compared to many solid tumors subscribing to the "Warburg effect" phenotype [9, 10]. Concordantly, prostate cancer cells showed a dominant uptake of fatty acids over glucose, with the uptake of palmitic acid measured at ~20 times higher than uptake of glucose in both malignant and benign prostate cancer cells [11]. Furthermore, exogenous fatty acids are readily oxidized by PCa, reducing glucose uptake [12]. Together, these studies demonstrate that exogenous uptake is a significant and previously underappreciated supply route of lipids in cancer cells with a lipogenic phenotype.

Both healthy and malignant prostate cells rely on androgens for a variety of physiological processes, including several metabolic signaling pathways. Androgens, through binding to the androgen receptor (AR), transcriptionally regulate a multitude of pathways, including proliferation, differentiation and cell survival of prostate cancer [13], with approximately equal numbers of genes activated and suppressed by androgen-activated AR. Targeting of the AR signaling axis is the mainstay treatment strategy for advanced prostate cancer. While initially effective in suppressing tumor growth, patients inevitably develop castrate-resistant prostate cancer (CRPC), which remains incurable. Importantly, during progression to CRPC,

Author Manuscript Published OnlineFirst on February 26, 2019; DOI: 10.1158/1541-7786.MCR-18-1147
Author manuscripts have been peer reviewed and accepted for publication but have not yet been edited.

survival and growth of prostate cancer cells remain dependent on AR activity, as demonstrated by treatment resistance mechanisms involving AR mutation, amplification and intratumoral steroidogenesis [reviewed in [14]]. Thus, identifying critical pathways regulated by AR might provide novel therapeutic strategies to combat development of CRPC. Lipogenesis is a well-described AR-regulated metabolic pathway that supports prostate cancer cell growth by providing fuel, membrane material and steroid hormone precursor (cholesterol). Androgens stimulate expression of FASN via activation of sterol regulatory element-binding proteins (SREBPs) [15], lipogenic enzymes ACACA and ACLY, and cholesterol synthesis enzymes HMGCS1 and HMGCR [3, 16]. In contrast, the role and expression of lipid transporters and their regulation by AR in prostate cancer remain largely uncharacterized [11, 17].

Our current understanding of lipid uptake is mostly derived from studies in non-malignant cells and tissues. The hydrophobic properties of lipids allow for passive, non-specific uptake via diffusion into the cell. Selective, protein-mediated lipid uptake involves receptor-mediated endocytosis of lipid transporters and their cognate lipoprotein cargo [18, 19] which contains various lipid components (phospholipids, cholesterol esters, triacylglycerol) that can be internalized via lipoprotein receptors (LDLR, VLDLR) or scavenger receptors (SCARB1, SCARB2). Various scavenger receptors have also been shown to be associated with uptake of modified (acetylated or oxidized) LDL particles, including SCARF1, SCARF2 and CXCL16 [20, 21]. Free fatty acids can be taken up by a family of six fatty acid transport proteins (SLC27A1-6) as well as fatty acid translocase (FAT/CD36) and GOT2/$FABP_{pm}$ [17].

Taken together, it is becoming evident that enhanced lipogenesis in prostate cancer development and progression is not the sole deregulated lipid supply pathway, and lipid uptake might play an important role in biochemical recurrence of prostate cancer. This

Author Manuscript Published OnlineFirst on February 26, 2019; DOI: 10.1158/1541-7786.MCR-18-1147
Author manuscripts have been peer reviewed and accepted for publication but have not yet been edited.

warranted a comprehensive investigation and delineation of lipid uptake and the lipid transporter landscape in prostate cancer as well as its regulation by AR.

Materials and methods

Cell culture

The following cell lines were acquired from American Type Culture Collection (ATCC) in 2010: LNCaP (CVCL_0395), C4-2B (CVCL_4784) and VCaP (CVCL_2235). Fibroblast-free DuCaP cells were a generous gift from M. Ness (VTT Technical Research Centre of Finland). LNCaP and C4-2B cells were cultured in Roswell Park Memorial Institute (RPMI) medium (Thermo Fisher Scientific) supplemented with 5% Fetal Bovine Serum (FBS) until passage 45. DuCaP and VCaP cells were cultured in RPMI supplemented with 10% FBS until passages 40 and 45, respectively. Medium was changed every 3-4 days. All cell lines were incubated at 37°C in 5% CO2. Cells were passaged at approximately 80% confluency by trypsinization. Cell lines were genotyped in March 2018 by Genomics Research Centre (Brisbane) and routinely tested for mycoplasma infection.

For androgen and anti-androgen treatments, cells were seeded in regular growth medium for 72 hours before media was replaced with RPMI supplemented with 5% CSS (Sigma-Aldrich). After 48 hours, media was replaced with fresh 5% CSS RPMI, and cells were treated with either dihydroxytestosterone (DHT, 10 nM) or synthetic androgen R1881 (1 nM) for 48 hours to activate AR signaling. AR-antagonist Enzalutamide or Bicalutamide (Selleck Chemicals, Houston, TX, USA) was used at 10 µM.

Measurement of lipid content by quantitative fluorescent microscopy

Prior to seeding of LNCaP and C4-2B cells in 5% CSS RPMI at a density of 4,000 and 3,000 cells/well, respectively, optical 96 well plates (IBIDI) were coated with 150 µl Poly-l-

ornithine (Sigma-Aldrich) as described previously [22]. DuCaP and VCaP cells were seeded in 10% CSS RPMI at a density of 15,000 cells/well. After treatment as indicated, media was removed, cells were washed with PBS once, fixed with 4% paraformaldehyde for 20 minutes at room temperature, and remaining aldehyde reacted with 30 mM glycine in PBS for an additional 30 minutes. Nuclear DNA was then stained with 1 µg/ml 4',6-diamidino-2-phenylindole (DAPI, Thermo Fisher Scientific) and lipids were stained with 0.1 µg/ml Nile Red (Sigma-Aldrich) overnight as described previously [23]. Alternatively, free cholesterol was stained with 50 µg/ml Filipin (Sigma-Aldrich) for 40 minutes. >500 cells/well were imaged using the InCell 2200 automated fluorescence microscope system (GE Healthcare Life Sciences). Quantitative analysis of 1500 cells/treatment (3 wells) was performed in at least two independent experiments with Cell Profiler Software (Broad Institute, [24]).

Measurement of lipid uptake by quantitative fluorescent microscopy

Cells were seeded as described above. For quantifying C16:0 fatty acid uptake, cells were treated growth media was exchanged with 65 µl/well of 0.2% BSA (lipid-free, Sigma-Aldrich) serum-free RPMI media supplemented with 5 µM Bodipy-C16:0 (Thermo-Fisher) and incubated at 37°C for one hour. Cellular uptake of cholesterol was measured as described recently [25]. Briefly, media was exchanged with serum-free 0.2% BSA RPMI media supplemented with 15 µM NBD cholesterol (22-(N-(7-Nitrobenz-2-Oxa-1,3-Diazol-4-yl) Amino-23,24-Bisnor-5-Cholen-3β-Ol) (Thermo-Fisher Scientific), and cells were incubated at 37°C for 2 hours. For quantifying lipoprotein complex uptake, serum-free 0.2% BSA RPMI media was supplemented with 1,1'-Dioctadecyl-3,3,3',3'-Tetramethylindocarbocyanine (DiI)-labelled acetylated-LDL (Thermo Fischer Scientific, 15µg/ml) or DiI-labelled LDL (Thermo Fisher Scientific, 15µg/ml) and incubated at 37°C for 2 hours. After incubation, cells were washed and fixed as described above. Cellular DNA and F-actin was

Author Manuscript Published OnlineFirst on February 26, 2019; DOI: 10.1158/1541-7786.MCR-18-1147
Author manuscripts have been peer reviewed and accepted for publication but have not yet been edited.

counterstained with DAPI and Alexa Fluor 647 Phalloidin (Thermo Fisher Scientific). Image acquisition and quantitative analysis were performed as above.

RNA extraction and quantitative real-time polymerase chain reaction (qRT-PCR)

Cells were seeded at a density of 9.0 x 10^4 (LNCaP and C4-2B) or 1.2x 10^5 (DuCaP and VCaP) cells/well in 6 well plates (ThermoScientific). Following completion of treatment, total RNA was isolated using the RNEasy mini kit (Qiagen) following the manufacturer's instructions. RNA concentration was measured using a NanoDrop ND-1000 Spectrophotometer (ThermoScientific), and RNA frozen at -80°C until further use.

Up to 2 µg of total RNA was used to prepare cDNA with SensiFast cDNA synthesis kit (Bioline) according to the manufacturer's instructions and diluted 1:5. qRT-PCR was performed with SYBR-Green Master Mix (Thermo Fisher Scientific) using the ViiA-7 Real-Time PCR system (Applied Biosystems). Determination of relative mRNA levels was calculated using the comparative ΔΔCt method [26], where expression levels were normalized relative to that of the housekeeping gene receptor-like protein 32 (*RPL32*) for each treatment and calculated as fold change relative to the vehicle control treatment. All experiments were performed independently in triplicate. Primer sequences are listed in supplementary materials.

Protein extraction and Western blot analysis

Proteins for western blotting were isolated by lysing cells in radio immunoprecipitation buffer [RIPA, 25 mM Tris, HCl pH 7.6, 150 mM NaCl, 1% NP-40, 1% sodium deoxycholate, 0.1% SDS, one cOmplete™ EDTA-free Protease Inhibitor Cocktail tablet (Roche) per 10 ml, phosphatase inhibitors NaF (30 µM), Sodium Pyrophosphate (20 µM), β-glycerophosphate (10 µM), and Na Vanadate (1 µM)]. With cells on ice, media was carefully removed and cells

Author Manuscript Published OnlineFirst on February 26, 2019; DOI: 10.1158/1541-7786.MCR-18-1147
Author manuscripts have been peer reviewed and accepted for publication but have not yet been edited.

were washed with PBS. RIPA lysis buffer was added, and cells were incubated for 5 minutes on ice before collection of protein lysates. Protein concentration was measured using Pierce BCA Protein Assay kit according to manufacturer's instructions (Thermo Fisher Scientific).

20 µg of total protein/lane were separated by SDS-polyacrylamide gel electrophoresis (SDS-PAGE) using NuPAGE™ 4-12% Bis-Tris SDS-PAGE Protein Gels (ThermoFisher Scientific), and Western blot was completed using the Bolt Mini Blot Module (Thermo Fisher Scientific) according to the manufacturer's instructions. Membranes were reacted over night at 4ºC with primary antibodies raised against LDLR (Abcam, ab52818) and SCARB1 (Abcam, ab217318) at a dilution of 1:1000 followed by probing with the appropriate Odyssey fluorophore-labelled secondary antibody and visualization on the LiCor® Odyssey imaging system (LI-COR® Biotechnology, NE, USA). Protein expression levels were quantified using Image Studio Lite (LI-COR® Biotechnology, NE, USA), normalized relative to the indicated housekeeping protein, and expressed as fold-changes relative to the control treatment.

Cistrome analysis of AR ChIPseq peaks

AR ChIPseq analysis used BED files (hg38) downloaded from Cistrome [27] for the +/- Bicalutamide treated vehicle controls for the ChIPseq dataset, GSE49832 [28]. The bedtools software tool (version 2.27.0) was used to identify AR ChIPseq peaks enriched in regions 5KB upstream and also in a 25KB window around Gencode transcripts (version 21).

RNA sequencing analysis

For mRNAseq, total cellular RNA was extracted using the Norgen RNA Purification PLUS kit #48400 (Norgen Biotek Corp., Thorold, Canada) according to the manufacturer's instructions, including DNase treatment. RNA quality and quantity were determined on an

Author Manuscript Published OnlineFirst on February 26, 2019; DOI: 10.1158/1541-7786.MCR-18-1147
Author manuscripts have been peer reviewed and accepted for publication but have not yet been edited.

Agilent 2100 Bioanalyzer (Agilent Technologies, Santa Clara, USA) and Qubit®. 2.0 Fluorometer (Thermo Fisher Scientific Inc, Waltham, USA). Library preparation and sequencing was done at the Kinghorn Centre for Clinical Genomics (KCCG, Garvan Institute, Sydney) using the Illumina TruSeq Stranded mRNA Sample Prep Kit with an input of 1 ug total RNA (RIN>8), followed by paired-end sequencing on an Illumina HiSeq2500 v4.0 (Illumina, San Diego, USA), multiplexing 6 samples per lane and yielding about 30M reads per sample. Raw data was processed through a custom designed pipeline. Raw reads were trimmed using 'TRIMGALORE' [29], followed by parallel alignments to the genome (hg38) and transcriptome (Ensembl v77 / Gencode v21) using the 'STAR' [30] aligner and read quantification with 'RSEM' [31]. Differential expression between two conditions was calculated after between sample TMM normalization [32] using 'edgeR' [33] (no replicates: Fisher Exact Test; replicates: General Linear Model) and is defined by an absolute fold change of >1.5 and an FDR corrected p-value <0.05. Quality control of raw data included sequential mapping to the ERCC spike-in controls, rRNA and a comprehensive set of pathogen genomes as well as detection and quantification of 3'bias. Heatmaps were generated with a hierarchical clustering algorithm using completed linkage and Euclidean distance measures.

Microarray gene expression profiling and analysis

RNA from LNCaP tumour xenograft models of CRPC were collected as described previously [34]. RNA was prepared for microarray profiling as described previously using a custom 180 K Agilent oligo microarray (VPCv3, ID032034, GEO:GPL16604) [35]. Probes significantly different between two groups were identified with an adjusted p-value of <=0.05, and an average absolute fold change of >=1.5 (adjusted for a false discovery rate (FDR) of 5%).

Statistical Analysis

Author Manuscript Published OnlineFirst on February 26, 2019; DOI: 10.1158/1541-7786.MCR-18-1147
Author manuscripts have been peer reviewed and accepted for publication but have not yet been edited.

Statistical analyses were performed with Graphpad Prism 7.0 (Graphpad Software, San Diego, CA) and R Studio (RStudio, Boston, MA). Data reported and appropriate statistical tests are included in figure legends.

Results

Androgens strongly increased cellular lipid content in AR-positive prostate cancer cells

Previous analysis by cellular Oil Red O staining and lipid chromatography of cellular extracts have demonstrated that androgens strongly enhance lipogenesis and cellular lipid content in prostate cancer cells, predominantly that of neutral lipids (triacylglycerols and cholesterol-esters) stored in lipid droplets and phospholipids and free cholesterol present in membranes [16, 36]. Consistent with these findings, our quantitative fluorescence microscopy (qFM) assay [23] of Nile Red-stained AR-positive prostate cancer cell lines LNCaP, C4-2B, VCaP and DuCaP showed that synthetic androgen R1881 significantly increased cellular phospholipid and neutral lipid content as well as lipid droplet number (Fig. 1). This stimulatory effect of androgen was also observed with DHT (Fig. S1) and mibolerone (data not shown) and blocked in the presence of Enzalutamide (Fig. S1). Furthermore, qFM of filipin-stained LNCaP cells confirmed that androgens also increased cellular levels of free, unesterified cholesterol (Fig. 1B), which was also blocked by Enzalutamide. While androgen-enhanced lipogenesis is a well characterized fuel source for increased cellular lipid content, the role of lipid uptake in this process is still poorly understood.

Fatty acid, cholesterol and lipoprotein uptake are increased by androgens

To directly measure the stimulatory effect of androgens on lipid uptake, a series of lipid uptake assays (Fig. 2) was used based on qFM of fluorophore labelled lipid probes (Bodipy-C16:0, NBD-cholesterol, DiI-LDL, and DiI-acetylated LDL). As shown in Figure 2A, androgen treatment (R1881) of four AR positive prostate cancer cell lines (LNCaP, C4-2B,

Author Manuscript Published OnlineFirst on February 26, 2019; DOI: 10.1158/1541-7786.MCR-18-1147
Author manuscripts have been peer reviewed and accepted for publication but have not yet been edited.

DuCaP, and VCaP) for 48 hours significantly increased uptake of Bodipy-C16:0. This effect was significantly blocked when cells were co-treated with Enzalutamide. Notably, androgens also increased uptake of Bodipy-C12:0 but not Bodipy-C5:0 (data not shown and Fig. S2), suggesting that cellular uptake of short chain fatty acids is not androgen regulated. Similar to fatty acid uptake, androgens also significantly increased uptake of NBD-cholesterol in AR-positive prostate cancer cells (Fig. 2B), and Enzalutamide significantly suppressed this effect. Representative images of LNCaP cells show that Bodipy-C16:0 and NBD-cholesterol were readily incorporated into lipid droplets (Fig. 2A and 2B)

The majority of serum lipids are transported as lipoprotein particles (chylomicrons, VLDL, LDL, HDL), containing a complex mixture of apolipoproteins, phospholipids, cholesterol and triacylglycerols which are taken up into cells by receptor-mediated endocytosis through cognate lipoprotein receptors such as the LDL receptor (LDLR) for LDL and scavenger receptor SCARB1 for acetylated LDL/HDL. Notably, in contrast to the covalent Bodipy and NBD fluorophore tags on C16:0 and cholesterol, the DiI label is a non-covalently bound dye infused into the lipoprotein particles that dissociates after cellular uptake and lysosomal processing. As shown in Figure 2C, androgens significantly enhanced uptake of DiI-complexed LDL and acetylated LDL in LNCaP cells in a dose-dependent manner, indicating a potential role their cognate receptors LDLR and SCARB1.

Androgen-enhanced lipid uptake is independent of cell cycle progression and proliferation

Androgen-mediated activation of AR promotes G0/G1 to S phase progression of the cell cycle and proliferation in prostate cancer cells [reviewed in [13, 37, 38]]. Because proliferation requires substantial membrane biogenesis for daughter cell generation, it was

Author Manuscript Published OnlineFirst on February 26, 2019; DOI: 10.1158/1541-7786.MCR-18-1147
Author manuscripts have been peer reviewed and accepted for publication but have not yet been edited.

possible that androgen-enhanced lipid uptake was not mediated directly through AR signaling but indirectly as a result of androgen-stimulated proliferation. To address this possibility, LNCaP cells were synchronized in G0/G1 (>95% of cell population, Fig. S3A) by incubation in CSS medium for 48 hours and treated for another 24 hours with three different cell cycle inhibitors, which upon androgen (DHT) treatment-induced re-entry into the cell cycle caused arrest in G0/G1 (Tunicamycin), S phase (Hydroxyurea) or G2/M (Nocodazole) (Fig. S3A). As shown in Figure 3, lipid uptake of Bodipy-C16:0 and NBD-cholesterol was significantly and to a similar magnitude enhanced by androgen in the presence of all three cell cycle inhibitors when compared to control. Flow cytometry of DNA content confirmed cell cycle arrest (Fig. S3B) by the inhibitors, and IncuCyte cell confluence analysis demonstrated growth inhibition (Fig. S3C), respectively. Thus, androgen regulation of lipid uptake is directly mediated by AR throughout the cell cycle and is independent of cell cycle progression and proliferation. Notably, a time course experiment of DHT-treated G0/G1 synchronized LNCaP cells in the presence of Tunicamycin (Fig. S3B, FACS) confirmed that the androgen-enhanced expression of classical AR-regulated genes *KLK3/PSA* (Fig. S3D), *TMPRSS2* and *FKBP5* (data not shown) remained unaffected under the experimental conditions.

Delineating the lipid transporter landscape in prostate cancer

While the role of genes involved in *de novo* lipogenesis (e.g. *ACLY, ACACA, FASN, HMGCR*) are well described in prostate cancer, and their overexpression is associated with tumor development, disease progression, aggressiveness, and poor prognosis, (reviewed in [1, 2], very little is known about the expression and functional importance of lipid transporters in prostate cancer, their regulation by androgens and their clinical relevance. To delineate the

Author Manuscript Published OnlineFirst on February 26, 2019; DOI: 10.1158/1541-7786.MCR-18-1147
Author manuscripts have been peer reviewed and accepted for publication but have not yet been edited.

lipid transporter landscape in prostate cancer, a panel of 44 candidate lipid transporters was generated based on previous work describing their lipid transport function in various human tissues [19, 39-44].

Transcriptomic analysis by RNAseq revealed that 41 candidate lipid transporters were expressed in five prostate cancer cell lines (LNCaP, DuCaP, VCaP, PC-3 and Du145) under normal culture conditions (a selection of 36 candidates are shown in Fig. 4A). Importantly, lipid transporters *LDLR*, *SCARB1*, *SCARB2*, and *GOT2/ FABP*$_{pm}$; were robustly expressed at levels comparable to lipogenic genes *HMGCR* and *FASN* (Fig. 4A), whereas seven transporters, including *CD36* and *SLC27A6* displayed FPKM values <1 in the majority of cell lines. In addition, mRNA expression of these 41 lipid transporters was independently detected in LNCaP and Du145 cells and six additional prostate cancer cell lines (CWR22RV1, EF1, H660, LASCPC-01, NB120914 and NE1_3) [[45], personal communication], verifying mRNA expression of these transporters in a total of nine prostate cancer cell lines. Comparison of this list of lipid transporters with the recently delineated plasma membrane proteome of eight prostate cancer cell lines, including LNCaP, Du145 and CWR22Rv1 [[45], personal communication] and previous work in LNCaP and CWR22Rv1 cells [17], confirmed the surface expression of LDLR, GOT2, LRPAP1, LRP8 and SCARB2. In addition, our proteomics analysis confirmed the exclusive expression of SCARB1, SCARB2, LRPAP1, SLCA27A1 and SLC27A2 in the membrane fraction of LNCaP cells, while GOT2 was also present in the soluble fraction (data not shown), which is consistent with its mitochondrial function. Western blot analysis demonstrated the expression of LDLR and SCARB1 in cell lysates of 7 malignant and 2 non-malignant prostate cell lines (Fig. 4B). Subsequently, expression of these lipid transporters in prostate cancer patient samples and clinical relevance was investigated by analyzing published tumor transcriptome datasets with Oncomine. Comparison of primary, localized prostate cancer versus normal prostate gland

Author Manuscript Published OnlineFirst on February 26, 2019; DOI: 10.1158/1541-7786.MCR-18-1147
Author manuscripts have been peer reviewed and accepted for publication but have not yet been edited.

revealed that mRNA levels of only a few lipid transporter were significantly ($p<0.05$) upregulated in primary prostate cancer and no lipid transporter was significantly downregulated (Fig. S4A-C). However data mining of the reported proteome analysis of primary prostate cancer versus neighboring non-malignant tissue [46] revealed that expression of 21 lipid transporters was lower in primary prostate cancer , whereas protein expression of both *de novo* lipogenesis enzymes FASN and HMGCR was increased by several magnitudes (Fig. S4D). Although a measurable degree of discordance between mRNA and protein levels has been previously noted in integrated transcriptome and proteome studies of prostate cancer [46, 47], the proteomics data suggested that lipid uptake is reduced and DNL is increased in primary prostate cancer when compared to normal prostate gland. In contrast, mRNA levels of several lipid transporters were significantly upregulated in metastatic tumor samples compared to primary site in the [48], including *SLC27A1*, *SLC27A3*, *SCARB1* and *LDLR* (Fig. 4C). Concordantly, analysis of the proteome comparison of localized prostate cancer versus bone metastasis [49] demonstrated that expression of 16 lipid transporters and FASN was higher in bone metastases (Fig. 4E), suggesting that tumor lipid supply from both uptake and DNL was increased. The lipoprotein transporters LDLR and SCARB1 were further investigated across other prostate cancer patient cohorts in Oncomine, including the Varambally [50] and La Tulippe [51] data sets. Both lipid transporter mRNAs were found to be significantly upregulated in samples from prostate cancer metastases when compared to primary tumors (Fig. 4E). Together, independently published data and our own analyses confirmed the mRNA, protein and plasma membrane expression of several lipid transporters in prostate cancer cell lines and patient-derived tumor samples. Importantly, our analysis demonstrated that this route of lipid supply is clinically significant during disease progression and is associated with metastasis to the bone.

Author Manuscript Published OnlineFirst on February 26, 2019; DOI: 10.1158/1541-7786.MCR-18-1147
Author manuscripts have been peer reviewed and accepted for publication but have not yet been edited.

Androgens regulate the expression of several lipid transporters

As shown above, androgens strongly enhance lipid uptake in AR-positive prostate cancer cell lines. However, our current understanding of the androgen receptor regulation of lipid transporters is very limited [17]. We initiated a comprehensive analysis of androgen-regulated lipid transporters by searching for AR binding sites within a 25 kb window of the gene sequence and a 5 kb window upstream of the protein start codon of 45 candidate lipid transporters in the reported AR ChIPseq data set of LNCaP cells treated with AR-antagonist Bicalutamide [28]. As shown in Figure 5A, 19 and 27 lipid transporters showed enrichment of AR ChIPseq peaks in the 5 kb and 25 kb windows, respectively, which was reduced in the presence of Bicalutamide. Consistent with its reported androgen-regulation [17], AR ChIPseq peaks were detected in the 25 kb window of the *GOT2* gene which were absent after Bicalutamide treatment. For comparison, AR-regulated lipogenesis genes *ACACA*, *FASN* and *HMGCR* [52] also showed reduced enrichment of AR ChIP peaks with Bicalutamide. Notably, lipid transporter genes might contain additional AR ChIP peaks outside the cut-off of 25 kb. Alternatively, the absence of AR ChIP peaks might indicate that they are indirectly regulated by androgen-activated transcription factors, e.g. sterol element binding proteins 1 and 2 (SREPB1/2). Indeed, the LDLR gene lacks AR ChIP peaks but contains flanking sterol regulatory elements and is positively regulated by SREBP1/2 [53, 54].

Next, mRNA transcript levels of our panel of 44 candidate lipid transporters were measured by RNAseq in three AR-positive, androgen-sensitive prostate cancer cell lines (LNCaP, DuCaP, VCaP) under conditions identical to the lipid content and uptake studies shown above (androgen deprivation in CSS for 48 hours and treatment with either vehicle or DHT (10 nM) for 48 hours). As a control, AR function was blocked with enzalutamide in the presence and absence of DHT. As shown in Figure 5B, RNAseq analysis demonstrated that expression of 36 lipid transporter genes was altered by androgen treatment in LNCaP cells.

Author Manuscript Published OnlineFirst on February 26, 2019; DOI: 10.1158/1541-7786.MCR-18-1147
Author manuscripts have been peer reviewed and accepted for publication but have not yet been edited.

Cholesterol efflux pump *ABCA1* and scavenger receptor *SCARF1* mRNA was significantly reduced by androgens, a response that was antagonized by Enzalutamide. In contrast, DHT significantly increased the expression of fatty acid transporters (*GOT2, SLC27A3, SLC27A4, SLC27A5, CD36*) and lipoprotein transporters (*LDLR, LRP8, SCARB1*) which was also blocked by Enzalutamide. Receptor-mediated endocytosis of lipoprotein particles through LDLR, VLDLR, SCARB1, SCARB2 and LDL receptor related proteins (LRP1-12, LRPAP1) converges in lysosomes for lipolysis and release of free cholesterol and fatty acids into the cytoplasm through their respective efflux pumps. Consistent with this, mRNA for lysosomal cholesterol efflux transporter NPC1 was also increased by DHT. Similar effects of DHT regulation of lipid transporter expression were observed in DuCaP and VCaP cells, with the exception of *SLC25A5*, *LRP8* and *SCARB1* which were repressed by DHT (Supplementary Figure S5A). qRT-PCR showed significantly increased mRNA expression of the lipoprotein transport receptors *LDLR* ($p<0.0001$) and *VLDLR* ($p<0.0001$) in LNCaP cells treated with 1 nM R1881 (Fig. 5C, top panel). While R1881 also enhanced expression of *SCARB1* and *SLC27A4*, there was no significant change in expression ($p>0.05$), although both showed similar trends to *LDLR* and *VLDLR* (Fig. 5C bottom panel). Co-treatment with Enzalutamide (10 µM) blocked the increase in lipid transporter expression (Fig. 5C). Analysis of DuCaP cells revealed similar results, demonstrating that the mRNA expression of the majority of tested lipid transporters was significantly enhanced by androgens (Fig. S5B). Western blot analysis demonstrated that LNCaP cells exposed to 10nM DHT showed an almost 2-fold increase in LDLR protein expression, which was suppressed to levels similar to vehicle control when co-treated with Enzalutamide (Fig. 5D, left panel). A similar trend of increased protein expression in cells treated with DHT was observed for SCARB1 (Fig. 5D, right panel). Cellular localization of LDLR protein in response to R1881 (1 nM) using immunofluorescent microscopy showed that androgen treatment resulted in significantly

Author Manuscript Published OnlineFirst on February 26, 2019; DOI: 10.1158/1541-7786.MCR-18-1147
Author manuscripts have been peer reviewed and accepted for publication but have not yet been edited.

increased expression of LDLR at the cellular periphery (plasma membrane, Fig.5E), which was blocked by Enzalutamide (10 µM), confirming that AR signaling enhanced the abundance of LDLR protein at the cell surface. Finally, review of our previously reported longitudinal LNCaP xenograft study [34] revealed that mRNA levels of *LDLR*, *VLDLR*, *SCARB1*, *SLC27A5* and *SLC27A6* were reduced seven days after castration (nadir) when compared to castration-naïve tumors (intact) (Fig 5F), which is consistent with their positive AR-regulation of expression in LNCaP cells *in vitro* shown above.

Discussion

Increased activation of *de novo* lipogenesis is a well-established metabolic phenotype in prostate cancer and other types of solid cancer, however therapeutic inhibition of DNL alone has so far had only limited clinical success as therapy against neoplastic disease. Targeting DNL in pre-clinical cancer models, including our own work in prostate cancer, demonstrated that inhibition of DNL leading to lipid starvation can be efficiently rescued by exogenous lipids [55]. Furthermore, obesity has been associated with more aggressive disease at diagnosis and higher rate of recurrence in prostate cancer patients [reviewed in [56, 57]]. Thus, exogenous lipids may play a much more significant role in prostate cancer and other types of cancer than previously acknowledged. Indeed, recent estimates derived from studies in lung cancer cells with a similar lipogenic phenotype as prostate cancer cells suggested that 70% of lipid carbon biomass is derived from exogenous lipids and only 30% from DNL [8]. While androgens are known to activate DNL in prostate cancer [58], little is known about lipid uptake in this context.

In this study we evaluated the effect of androgen treatment on lipid content (free cholesterol, neutral and phospholipids and lipid droplets) and lipid uptake of several lipid probes (C5:0, C12:0 and C16:0 fatty acids, cholesterol, LDL and acetylated LDL) in a panel of prostate cancer cells. By applying cutting-edge automated quantitative fluorescence microscopy and

image analysis, we provide the functionally most comprehensive analysis of lipid uptake in prostate cancer cells to date. Our work demonstrates that androgen significantly enhanced cellular uptake of LDL particles as well as free fatty acids and cholesterol and their subcellular storage in lipid droplets. Consistent with this, we showed a concordant increase in cellular phospholipids (membrane), neutral lipids (cholesterol-FA esters and TAGs stored in lipid droplets) and free cholesterol (Fig. 1A-B), which is a major component of cell membranes and essential for membrane structure and functional organization as well as a precursor for steroidogenesis reviewed in [59]. While our work did not delineate the relative contributions of various anabolic and catabolic lipid metabolism processes to the net increase in cellular lipid content in response to androgen treatment, e.g. enhanced lipid uptake and lipogenesis [58] versus fatty acid oxidation, phospholipid degradation, steroidogenesis and lipid efflux, it nevertheless shows that androgens caused a strong and expansive increase in lipid uptake across various lipid species. Our ongoing work suggests that lipid uptake has a higher supply capacity than DNL in prostate cancer cells (data not shown) which is consistent with the ability of exogenous lipids to efficiently recue DNL inhibition [55] and recent work estimating that 70% of carbon lipid biomass is derived from exogenous lipids in lung cancer cells expressing the lipogenic phenotype [8]. Critically, we demonstrated that androgen-enhanced lipid uptake is directly mediated by AR signaling and independent of its stimulatory effect on cell cycle progression and proliferation [13, 37], i.e. androgen-enhanced fatty acid and cholesterol uptake remained unaffected in prostate cancer cells arrested in G0/G1, S phase or G2/M and in the absence of cell growth. This suggests that AR-regulated lipid uptake is maintained throughout the cell cycle, is not part of a cell cycle specific AR subnetwork [60] and is not indirectly caused by lipid biomass demand of daughter cell generation.

Importantly, this work for the first time comprehensively elucidated the lipid transporter landscape in prostate cancer. Recent integrative omics studies of prostate cancer patient samples highlighted a measurable degree of discordance between genomics, epigenetics, transcriptomics and proteomics, i.e., that gene copy number, DNA methylation and mRNA levels did not reliably predict proteomic changes [46, 47]. In addition, the plasma membrane localization of most candidate lipid transporters remains to be confirmed in prostate cancer [17, 61] despite recent progress in overcoming technical limitations challenging the comprehensive delineation of the surface proteome of prostate cancer cells [45]. By comparing transcriptomic and proteomic analyses of cell lines, tumor xenografts and patient samples, our work has conclusively demonstrated robust mRNA expression of 34 lipid transporters in multiple prostate cancer cell lines and expression of six lipid transporter proteins in the membrane fraction of LNCaP cells, of which plasma membrane expression was independently confirmed for LDLR, GOT2, LRPAP1, LRP8 and SCARB2 in eight prostate cancer cell lines [17, 45], personal communication]. Our data mining of previously reported prostate cancer tumor proteomes (normal gland vs primary prostate cancer and primary prostate cancer vs bone metastasis, [46, 49] demonstrated that the expression of the lipid transporter landscape substantial changes during prostate cancer progression from localized disease (21 lipid transporters downregulated=low lipid uptake) to bone metastatic disease (16 lipid transporters upregulated=high lipid uptake). For comparison, the enhanced expression of lipogenic enzymes suggested that lipid synthesis was upregulated throughout prostate cancer progression from primary to metastatic disease. Our Oncomine analysis revealed a similar trend in the mRNA expression of lipid transporters in three prostate cancer patient sample cohorts reported previously (Grasso 2012, Varambally 2005, La Tulippe 2002). If, and to what extent, the extremely lipid-rich environment of the bone marrow (50-70% adiposity in adult men [62] is associated with enhanced lipid uptake in prostate cancer

Author Manuscript Published OnlineFirst on February 26, 2019; DOI: 10.1158/1541-7786.MCR-18-1147
Author manuscripts have been peer reviewed and accepted for publication but have not yet been edited.

bone metastases remains to be investigated, including the possibility that the increased incidence of prostate cancer metastases to bone is linked to high levels of adiposity and specific lipid species within bone marrow which provide increased stimulus for more aggressive growth and pro-tumorgenic lipid signaling of metastatic prostate cancer. Of the 22 bone metastasis proteomes that were analyzed, 16 were from patients after long-term ADT and classified as CRPC, with one short-term ADT and five hormone-naïve cases, yet all shared the same general features, including enhanced lipid transport and fatty acid oxidation [49], suggesting that castration-resistant bone metastases rely on similar mechanisms for growth as hormone-naïve metastatic bone tumors. Contrary to above reports, an integrated transcriptomics and lipidomics study highlighted increased mRNA levels of *SCARB1*, *GOT2* and *SLC27As 2*, *4* and *5* as well as polyunsaturated fatty acid (PUFA) accumulation in 20 paired localized primary tumors compared to matched adjacent non-malignant prostate tissue [63]. While PUFA synthesis from essential fatty acids α -linolenic acid and linoleic acids remained transcriptionally unchanged, the authors proposed that increased phospholipid uptake through SCARB1 caused intratumoral PUFA enrichment in localized prostate cancer; however, this hypothesis still awaits experimental confirmation. The reason for discordance between both studies regarding lipid uptake in localized prostate cancer is unclear, but it is noteworthy that the activity of lipid transporters is also regulated through changes in their subcellular localization, highlighting the need for an integrated analysis of the cell surface proteome and tumor lipidome in prostate cancer. We conclude that LDLR, GOT2, LRPAP1, LRP8, SCARB1 and SCARB2 are high confidence lipid transporters that are associated with prostate cancer disease progression and bone metastasis, but further work is needed to fully delineate the lipid transporter proteome at the plasma membrane in prostate cancer.

We have provided the most comprehensive functional analysis of lipid uptake in prostate cancer cells to date and demonstrated that androgens strongly enhanced lipid uptake of fatty

acids, cholesterol and lipoprotein particles LDL and acetylated LDL in AR-positive prostate cancer cell lines (summarized in Fig. 6). Previous work indicated that expression of GOT2/FABPpm is enhanced by androgens and increases the cellular uptake of medium and long chain fatty acids in LNCaP and CWR22Rv1 prostate cancer cells [17]. Our comprehensive analyses of AR binding sites (ChIPseq peaks), RNAseq (of three DHT-treated AR-positive prostate cancer cell lines), qRT-PCR, Western blot and DNA microarray of LNCaP tumor xenograft [34] revealed that an equal number of lipid transporters are activated and suppressed by androgens. AR-negative malignant and non-malignant prostate cell lines (PC-3, Du145 and BHP-1) show avid lipid uptake (data not shown) and expression of transporters (Fig. 4A-B). Thus, it is likely that other signaling pathways regulate lipid supply in these cell lines. Furthermore, after using the independently confirmed plasma membrane expression [45] as a high confidence filter, we conclude that LRPAP1 and SCARB2 are androgen-suppressed and LRP8, SCARB1, LDLR and GOT2 are androgen-enhanced surface lipid transporters in prostate cancer cells. Interestingly, GOT2 (mitochondrial aspartate aminotransferase) is better known for its role in amino acid metabolism, the cytoplasm-mitochondria malate-aspartate shuttle, and the urea and tricarboxylic acid cycles**.** This suggests that moonlighting of metabolic enzymes in other subcellular compartments [64], e.g., the plasma membrane [17, 61] and strikingly, with additional substrate specificities and catalytic activity [65]. Thus, there is a possibility that future studies will discover additional proteins involved in lipid uptake due to their plasma membrane expression.

Targeting cholesterol homeostasis in prostate cancer as a therapeutic strategy to delay development of CRPC has recently received increasing attention [66-68]. Cholesterol is a precursor of steroid hormone synthesis, and we previously showed that progression to CRPC is associated with increased intratumoral steroidogenesis of androgens [34]. Hypercholesterolemia has been reported to enhance LNCaP tumor xenograft growth and

intratumoral androgen synthesis [69], and monotherapy against dietary cholesterol adsorption in the intestine with ezetimibe [67] or *de novo* cholesterol synthesis with simvastatin [66] reduced LNCaP tumor xenograft growth, androgen steroidogenesis and delayed development of CRPC. Furthermore, targeting cholesterol uptake via SCARB1 antagonism with ITX5061, reduced HDL uptake (but not LDL) in LNCaP, VCaP and CRW22Rv1 cells and sensitized CWR22Rv1 tumor orthografts to ADT [68]. Comparatively, the same study showed that ITX5061 conferred stronger growth inhibition than simvastatin in LNCaP and CWR22Rv1 cells [68] under hormone-deprived conditions, suggesting that cholesterol uptake via SCARB1 is a significant supply route in this prostate cancer model. Due to the co-expression of multiple lipoprotein transporters (LDLR, VLDLR, SCARB1, LRP1-12) in conjunction with increased cholesterol synthesis in prostate cancer , novel co-targeting strategies antagonizing this cholesterol supply redundancy might have profound synergies in extending the efficacy of ADT and delaying the development of CRPC. Such co-treatment strategies could include simvastatin in combination with specific inhibitors of lipid processing in the lysosome, which is a critical hub for lipid uptake through endocytosis, including phagocytosis, pinocytosis and receptor-mediated endocytosis. The latter pathway is used by all major lipoprotein receptors, including LDLR, VLDLR, SCARB1 and the LRPs 1-12, and focus of a recently started Phase I/II clinical trial (NCT03513211). Strategies of co-targeting lipid uptake and synthesis with repurposed drugs are currently under investigation by our group and show very promising and potent anti-neoplastic synergies in pre-clinical models of advanced prostate cancer.

References

1. Swinnen, J.V., K. Brusselmans, and G. Verhoeven, *Increased lipogenesis in cancer cells: new players, novel targets.* Curr Opin Clin Nutr Metab Care, 2006. **9**(4): p. 358-65.
2. Menendez, J.A. and R. Lupu, *Fatty acid synthase and the lipogenic phenotype in cancer pathogenesis.* Nat Rev Cancer, 2007. **7**(10): p. 763-777.

3. Fritz, V., et al., *Abrogation of De novo Lipogenesis by Stearoyl-CoA Desaturase 1 Inhibition Interferes with Oncogenic Signaling and Blocks Prostate Cancer Progression in Mice.* Molecular Cancer Therapeutics, 2010. **9**(6): p. 1740-1754.
4. Deep, G. and I. Schlaepfer, *Aberrant Lipid Metabolism Promotes Prostate Cancer: Role in Cell Survival under Hypoxia and Extracellular Vesicles Biogenesis.* International Journal of Molecular Sciences, 2016. **17**(7): p. 1061.
5. Flavin, R., G. Zadra, and M. Loda, *Metabolic alterations and targeted therapies in prostate cancer.* The Journal of pathology, 2011. **223**(2): p. 283-294.
6. Kuemmerle, N.B., et al., *Lipoprotein lipase links dietary fat to solid tumor cell proliferation.* Mol Cancer Ther, 2011. **10**(3): p. 427-36.
7. Griffiths, B., et al., *Sterol regulatory element binding protein-dependent regulation of lipid synthesis supports cell survival and tumor growth.* Cancer & Metabolism, 2013. **1**: p. 3-3.
8. Hosios, Aaron M., et al., *Amino Acids Rather than Glucose Account for the Majority of Cell Mass in Proliferating Mammalian Cells.* Developmental Cell, 2016. **36**(5): p. 540-549.
9. Effert, P.J., et al., *Metabolic Imaging of Untreated Prostate Cancer by Positron Emission Tomography with sup 18 Fluorine-Labeled Deoxyglucose.* The Journal of Urology, 1996. **155**(3): p. 994-998.
10. Zadra, G., C. Photopoulos, and M. Loda, *The fat side of Prostate Cancer.* Biochimica et biophysica acta, 2013. **1831**(10): p. 1518-1532.
11. Liu, Y., L.S. Zuckier, and N.V. Ghesani, *Dominant uptake of fatty acid over glucose by prostate cells: a potential new diagnostic and therapeutic approach.* Anticancer Res, 2010. **30**(2): p. 369-74.
12. Schlaepfer, I.R., et al., *Inhibition of Lipid Oxidation Increases Glucose Metabolism and Enhances 2-Deoxy-2-[(18)F]Fluoro-D-Glucose Uptake in Prostate Cancer Mouse Xenografts.* Molecular imaging and biology : MIB : the official publication of the Academy of Molecular Imaging, 2015. **17**(4): p. 529-538.
13. Lonergan, P.E. and D.J. Tindall, *Androgen receptor signaling in prostate cancer development and progression.* Journal of Carcinogenesis, 2011. **10**: p. 20.
14. Dutt, S.S. and A.C. Gao, *Molecular mechanisms of castration-resistant prostate cancer progression.* Future oncology (London, England), 2009. **5**(9): p. 1403-1413.
15. Heemers, H., et al., *Identification of an androgen response element in intron 8 of the sterol regulatory element-binding protein cleavage-activating protein gene allowing direct regulation by the androgen receptor.* J Biol Chem, 2004. **279**(29): p. 30880-7.
16. Swinnen, J.V., et al., *Androgens markedly stimulate the accumulation of neutral lipids in the human prostatic adenocarcinoma cell line LNCaP.* Endocrinology, 1996. **137**(10): p. 4468-74.
17. Pinthus, J.H., et al., *Androgen-dependent regulation of medium and long chain fatty acids uptake in prostate cancer.* Prostate, 2007. **67**(12): p. 1330-8.
18. Sahoo, S., et al., *Membrane transporters in a human genome-scale metabolic knowledgebase and their implications for disease.* Frontiers in Physiology, 2014. **5**: p. 91.
19. Doege, H. and A. Stahl, *Protein-Mediated Fatty Acid Uptake: Novel Insights from In Vivo Models.* Physiology, 2006. **21**(4): p. 259-268.
20. Tamura, Y., et al., *Scavenger receptor expressed by endothelial cells I (SREC-I) mediates the uptake of acetylated low density lipoproteins by macrophages stimulated with lipopolysaccharide.* J Biol Chem, 2004. **279**(30): p. 30938-44.
21. Miller, Y.I., et al., *Lipoprotein Modification and Macrophage Uptake: Role of Pathologic Cholesterol Transport in Atherogenesis*, in *Cholesterol Binding and Cholesterol Transport Proteins: Structure and Function in Health and Disease*, J.R. Harris, Editor. 2010, Springer Netherlands: Dordrecht. p. 229-251.
22. Liberio, M.S., et al., *Differential effects of tissue culture coating substrates on prostate cancer cell adherence, morphology and behavior.* PLoS One, 2014. **9**(11): p. e112122.

23. Levrier, C., et al., *Denhaminols A-H, dihydro-beta-agarofurans from the endemic Australian rainforest plant Denhamia celastroides.* J Nat Prod, 2015. **78**(1): p. 111-9.
24. Kamentsky, L., et al., *Improved structure, function and compatibility for CellProfiler: modular high-throughput image analysis software.* Bioinformatics, 2011. **27**(8): p. 1179-1180.
25. Egbewande, F.A., et al., *Identification of Gibberellic Acid Derivatives That Deregulate Cholesterol Metabolism in Prostate Cancer Cells.* Journal of Natural Products, 2018. **81**(4): p. 838-845.
26. Schmittgen, T.D. and K.J. Livak, *Analyzing real-time PCR data by the comparative C(T) method.* Nat Protoc, 2008. **3**(6): p. 1101-8.
27. Mei, S., et al., *Cistrome Data Browser: a data portal for ChIP-Seq and chromatin accessibility data in human and mouse.* Nucleic Acids Res, 2017. **45**(D1): p. D658-D662.
28. Ramos-Montoya, A., et al., *HES6 drives a critical AR transcriptional programme to induce castration-resistant prostate cancer through activation of an E2F1-mediated cell cycle network.* EMBO Molecular Medicine, 2014. **6**(5): p. 651-661.
29. Krueger, F., 2012.
30. Dobin, A., et al., *STAR: ultrafast universal RNA-seq aligner.* Bioinformatics, 2013. **29**(1): p. 15-21.
31. Li, B. and C.N. Dewey, *RSEM: accurate transcript quantification from RNA-Seq data with or without a reference genome.* BMC Bioinformatics, 2011. **12**: p. 323.
32. Robinson, M.D. and A. Oshlack, *A scaling normalization method for differential expression analysis of RNA-seq data.* Genome Biol, 2010. **11**(3): p. R25.
33. Robinson, M.D., D.J. McCarthy, and G.K. Smyth, *edgeR: a Bioconductor package for differential expression analysis of digital gene expression data.* Bioinformatics, 2010. **26**(1): p. 139-40.
34. Locke, J.A., et al., *Androgen levels increase by intratumoral de novo steroidogenesis during progression of castration-resistant prostate cancer.* Cancer Res, 2008. **68**(15): p. 6407-15.
35. Sieh, S., et al., *Phenotypic Characterization of Prostate Cancer LNCaP Cells Cultured within a Bioengineered Microenvironment.* PLOS ONE, 2012. **7**(9): p. e40217.
36. Swinnen, J.V., et al., *Androgens stimulate fatty acid synthase in the human prostate cancer cell line LNCaP.* Cancer Res, 1997. **57**(6): p. 1086-90.
37. Heinlein, C.A. and C. Chang, *Androgen Receptor in Prostate Cancer.* Endocrine Reviews, 2004. **25**(2): p. 276-308.
38. Balk, S.P. and K.E. Knudsen, *AR, the cell cycle, and prostate cancer.* Nuclear Receptor Signaling, 2008. **6**: p. e001.
39. Anderson, C.M. and A. Stahl, *SLC27 fatty acid transport proteins.* Molecular aspects of medicine, 2013. **34**(2-3): p. 516-528.
40. Goldstein, J.L., R.G. Anderson, and M.S. Brown, *Receptor-mediated endocytosis and the cellular uptake of low density lipoprotein.* Ciba Found Symp, 1982(92): p. 77-95.
41. Go, G.-w. and A. Mani, *Low-Density Lipoprotein Receptor (LDLR) Family Orchestrates Cholesterol Homeostasis.* The Yale Journal of Biology and Medicine, 2012. **85**(1): p. 19-28.
42. Wang, M.-D., et al., *Different cellular traffic of LDL-cholesterol and acetylated LDL-cholesterol leads to distinct reverse cholesterol transport pathways.* Journal of Lipid Research, 2007. **48**(3): p. 633-645.
43. Kennedy, B.E., M. Charman, and B. Karten, *Niemann-Pick Type C2 protein contributes to the transport of endosomal cholesterol to mitochondria without interacting with NPC1.* Journal of Lipid Research, 2012. **53**(12): p. 2632-2642.
44. Nath, A. and C. Chan, *Genetic alterations in fatty acid transport and metabolism genes are associated with metastatic progression and poor prognosis of human cancers.* Sci Rep, 2016. **6**: p. 18669.

45. Lee, J.K., et al., *Systemic surfaceome profiling identifies target antigens for immune-based therapy in subtypes of advanced prostate cancer.* Proceedings of the National Academy of Sciences, 2018.
46. Iglesias-Gato, D., et al., *The Proteome of Primary Prostate Cancer.* European Urology, 2016. **69**(5): p. 942-952.
47. Latonen, L., et al., *Integrative proteomics in prostate cancer uncovers robustness against genomic and transcriptomic aberrations during disease progression.* Nat Commun, 2018. **9**(1): p. 1176.
48. Grasso, C.S., et al., *The mutational landscape of lethal castration-resistant prostate cancer.* Nature, 2012. **487**.
49. Iglesias-Gato, D., et al., *The proteome of prostate cancer bone metastasis reveals heterogeneity with prognostic implications.* Clinical Cancer Research, 2018.
50. Varambally, S., et al., *Integrative genomic and proteomic analysis of prostate cancer reveals signatures of metastatic progression.* Cancer Cell, 2005. **8**(5): p. 393-406.
51. LaTulippe, E., et al., *Comprehensive gene expression analysis of prostate cancer reveals distinct transcriptional programs associated with metastatic disease.* Cancer Res, 2002. **62**(15): p. 4499-506.
52. Swinnen, J.V., et al., *Coordinate regulation of lipogenic gene expression by androgens: evidence for a cascade mechanism involving sterol regulatory element binding proteins.* Proc Natl Acad Sci U S A, 1997. **94**(24): p. 12975-80.
53. Yokoyama, C., et al., *SREBP-1, a basic-helix-loop-helix-leucine zipper protein that controls transcription of the low density lipoprotein receptor gene.* Cell, 1993. **75**(1): p. 187-97.
54. Streicher, R., et al., *SREBP-1 mediates activation of the low density lipoprotein receptor promoter by insulin and insulin-like growth factor-I.* J Biol Chem, 1996. **271**(12): p. 7128-33.
55. Sadowski, M.C., et al., *The fatty acid synthase inhibitor triclosan: repurposing an anti-microbial agent for targeting prostate cancer.* Oncotarget, 2014. **5**(19): p. 9362-81.
56. Balaban, S., et al., *Obesity and Cancer Progression: Is There a Role of Fatty Acid Metabolism?* BioMed Research International, 2015. **2015**: p. 274585.
57. Taylor, R.A., et al., *Linking obesogenic dysregulation to prostate cancer progression.* Endocrine Connections, 2015. **4**(4): p. R68-R80.
58. Swinnen, J.V., et al., *Androgens markedly stimulate the accumulation of neutral lipids in the human prostatic adenocarcinoma cell line LNCaP.* Endocrinology, 1996. **137**(10): p. 4468-4474.
59. Subczynski, W.K., et al., *High Cholesterol/Low Cholesterol: Effects in Biological Membranes: A Review.* Cell Biochemistry and Biophysics, 2017. **75**(3): p. 369-385.
60. McNair, C., et al., *Cell-cycle coupled expansion of AR activity promotes cancer progression.* Oncogene, 2017. **36**(12): p. 1655-1668.
61. Stump, D.D., S.L. Zhou, and P.D. Berk, *Comparison of plasma membrane FABP and mitochondrial isoform of aspartate aminotransferase from rat liver.* American Journal of Physiology-Gastrointestinal and Liver Physiology, 1993. **265**(5): p. G894-G902.
62. Blebea, J.S., et al., *Structural and Functional Imaging of Normal Bone Marrow and Evaluation of Its Age-Related Changes.* Seminars in Nuclear Medicine, 2007. **37**(3): p. 185-194.
63. Li, J., et al., *Integration of lipidomics and transcriptomics unravels aberrant lipid metabolism and defines cholesteryl oleate as potential biomarker of prostate cancer.* Scientific Reports, 2016. **6**: p. 20984.
64. Boukouris, A.E., S.D. Zervopoulos, and E.D. Michelakis, *Metabolic Enzymes Moonlighting in the Nucleus: Metabolic Regulation of Gene Transcription.* Trends in Biochemical Sciences, 2016. **41**(8): p. 712-730.
65. Bradbury, M.W., et al., *MOLECULAR MODELING AND FUNCTIONAL CONFIRMATION OF A PREDICTED FATTY ACID BINDING SITE OF MITOCHONDRIAL ASPARTATE AMINOTRANSFERASE.* Journal of molecular biology, 2011. **412**(3): p. 412-422.

66. Gordon, J.A., et al., *Oral simvastatin administration delays castration-resistant progression and reduces intratumoral steroidogenesis of LNCaP prostate cancer xenografts.* Prostate Cancer Prostatic Dis, 2016. **19**(1): p. 21-7.
67. Allott, E.H., et al., *Serum cholesterol levels and tumor growth in a PTEN-null transgenic mouse model of prostate cancer.* Prostate Cancer Prostatic Dis, 2018. **21**(2): p. 196-203.
68. Patel, R., et al., *Sprouty2 loss-induced IL6 drives castration-resistant prostate cancer through scavenger receptor B1.* EMBO Mol Med, 2018. **10**(4).
69. Mostaghel, E.A., et al., *Impact of circulating cholesterol levels on growth and intratumoral androgen concentration of prostate tumors.* PLoS One, 2012. **7**(1): p. e30062.

Authors' Contributions

Conception and design: Martin C Sadowski, Kaylyn D Tousignant

Development of methodology: Martin C Sadowski, Kaylyn D Tousignant, Anja Rockstroh, Melanie L Lehman, Stephen J McPherson Nenad Bartonicek, Marcel E Dinger, Colleen C Nelson

Acquisition of data: Martin C Sadowski, Kaylyn D Tousignant, Anja Rockstroh, Stephen J McPherson, Lisa K Philp, Nenad Bartonicek, Marcel E Dinger

Analysis and interpretation of data (i.e. RNAseq analysis, computational analysis): Martin C Sadowski, Kaylyn D Tousignant, Anja Rockstroh, Atefeh Taherian Fard, Melanie Lehman, Chenwei Wang, Lisa K Philp, Colleen C Nelson

Writing, review, and/or revision of the manuscript: Martin C Sadowski, Kaylyn D Tousignant, Lisa K Philp, Atefeh Taherian Fard, Melanie Lehman, Steven J McPherson, Colleen C Nelson

Acknowledgements

This study was supported by the Movember Foundation and the Prostate Cancer Foundation of Australia through a Movember Revolutionary Team Award (K. Tousignant, A. Rockstroh, A. Fard, M. Lehman, C. Wang, S. McPherson, L. Philp, C. Nelson, M. Sadowski) and the Wang, S. McPherson, L. Philp, C. Nelson, M. Sadowski

Author Manuscript Published OnlineFirst on February 26, 2019; DOI: 10.1158/1541-7786.MCR-18-1147
Author manuscripts have been peer reviewed and accepted for publication but have not yet been edited.

Figure Legends

Figure 1: Androgens strongly increased lipid content of AR-positive prostate cancer cell lines. (A) LNCaP, C4-2B, VCaP and DuCaP cells were grown in charcoal-dextran stripped serum (CSS) for 48 hours and treated with 1 nM R1881 or vehicle (Ctrl) for 48 hours. Fixed cells were stained with fluorescent lipid stain Nile Red, and cellular mean fluorescent intensities (MFI) of phospholipid content (top left panel) and neutral lipid content (top right panel) as well as mean cellular number of lipid droplets (bottom left panel) and mean total cellular area of lipid droplets (bottom right panel) were measured by quantitative fluorescence microscopy (qFM). Representative 40x images of LNCaP cell are shown (blue=DNA, yellow=lipid droplets containing neutral lipids, scale bar=20 µm). (B) LNCaP cells were grown as described in (A) and treated with the indicated androgens in the presence or absence of Enzalutamide (Enz, 10 µM). Fixed cells were stained with Filipin to label free, unesterified cholesterol, and MFI of cellular free cholesterol was measured by qFM. (n~3000 cells from 3 wells; significance calculated relative to vehicle (Ctrl): ns=not significant, ***$p<0.001$, **$p<0.01$ *$p<0.05$ or vehicle-treated LNCaP cells: #$p<0.001$, representative of 3 independent experiments). Representative 40x images of LNCaP cell are shown (blue=DNA, green=free cholesterol, scale bar=10 µm).

Figure 2: Androgens strongly increased lipid uptake. (A) To measure fatty acid uptake, indicated cell lines were grown in CSS for 48 hours and treated with 1 nM R1881 in the presence or absence of Enz (10 µM) or vehicle (Ctrl) for 48 hours. Before fixation, cells were incubated with Bodipy-C16:0 for one hour and lipid uptake was measured by qFM (n~3000 cells from 3 wells, mean±SD, One-way ANOVA with Dunnett's multiple comparisons test relative to cell line specific control (Ctrl), ns=not significant, ***$p<0.001$, representative of 2 independent experiments). Representative 40x images of DuCaP cell are shown (blue=DNA,

red=F-actin, green=lipid droplets containing C16:0-Bodipy, scale bar=20 µm). (B) To measure cholesterol uptake, LNCaP cells were grown in CSS for 48 hours and treated with either 1 nM R1881 or 10 nM DHT in the presence or absence of ENZ (10 µM). Before fixation, cells were incubated with NBD-cholesterol for 2 hours and cellular levels were measured by qFM (n~3000 cells from 3 wells, mean±SD, One-way ANOVA with Dunnett's multiple comparisons test relative to cell line specific vehicle (Ctrl), or unpaired t test between androgen treatment alone or in combination with Enzalutamide, ns=not significant, ****p<0.0001, representative of 2 independent experiments). Representative 40x images of LNCaP cell are shown (blue=DNA, red=F-actin, green=lipid droplets containing NBD-cholesterol, scale bar=20 µm). (C) To measure lipoprotein uptake, LNCaP cells were grown in CSS for 48 h and treated with increasing concentrations of DHT or 1 nM R1881. Before fixation, cells were incubated with DiI-LDL or DiI-acLDL for 2 hours and lipoprotein uptake was measured by qFM (n~3000 cells from 3 wells, mean±SD, One-way ANOVA with Dunnett's multiple comparisons test relative to control (Ctrl) in each respective cell line, ****p<0.0001, representative of 3 independent experiments).

Figure 3: Androgen-enhanced lipid uptake is independent of cell cycle progression and proliferation. (A) LNCaP cells were synchronized in G0/G1 by androgen deprivation (CSS for 48 h) followed by treatment with Tunicamycin (1 mg/mL), Hydroxyurea (1 M), or Nocodazole (25 ug/mL) for another 24 h, placing cell cycle blocks in G0/G1, S phase and mitosis, respectively. Cell cycle re-entry and progression to the respective cell cycle block was stimulated by DHT (10 nM). After 24 h, cholesterol (NBD-Cholesterol, left panel) and fatty acid uptake (Bodipy-C16:0, right panel) was measured by qFM. (n~3000 cells from 3 wells, mean±SD, One-way ANOVA with Dunnett's multiple comparisons test relative to cell line specific vehicle (Ctrl), or unpaired t test between androgen treatment alone or in

Author Manuscript Published OnlineFirst on February 26, 2019; DOI: 10.1158/1541-7786.MCR-18-1147
Author manuscripts have been peer reviewed and accepted for publication but have not yet been edited.

combination with cell cycle inhibitor, ns=not significant, ****p<0.0001, **<0.01, representative of 2 independent experiments).

Figure 4: Delineation of the lipid transporter landscape in prostate cancer (A) mRNA expression levels (mean FPKM= fragments per kilobase million, n=2) of the indicated candidate lipid transporters and 2 lipogenic genes (*FASN* and *HMGCR*) were measured by RNAseq in the five indicated prostate cancer cell lines grown in their respective maintenance media. (B) Western blot confirmed the protein expression of LDLR and SCARB1 in the seven indicated prostate cancer cell lines and in two non-malignant prostate cell lines (RWPE-1, BHP-1) grown in their respective maintenance media. GAPDH was used as a loading control. A representative blot of two independent experiments is shown. (C) Oncomine analysis of candidate lipid transporters in Grasso dataset [48] comparing gene expression of localized, primary prostate cancer versus metastatic prostate cancer . (D) Protein expression analysis of indicated 18 lipid transporters and two lipogenesis enzymes (FASN and HMGCR) in paired patient samples of localized primary tumor and (blue) and bone metastasis (red) in the Iglesias-Gato proteome data set [49]. (E) Gene expression of *LDLR* (top panel) and *SCARB1* (bottom panel) was compared in primary vs metastatic prostate cancer in Grasso, Varambally and LaTulippe cohorts (mean±SD, unpaired t test, ns=not significant, ****p<0.0001, ***p<0.001, **<0.01, *p<0.05).

Figure 5: Androgens regulated the expression of lipid transporters. (A) AR ChIPseq peak enrichment analysis of 42 lipid transporter genes and six lipogenesis genes (*ACLY*, *ACSS2*, *ACACA*, *FASN*, *HMGCS1*, *HMGCR*) in the Ramos-Montoya data set of LNCaP cells treated with Bicalutamide (BIC) compared to vehicle control (VEH, [28]. The number of peaks is highlighted by the bubble size and the enrichment score by the gray scale. (B) LNCaP cells were grown in CSS for 48 hours and treated with 10 nM DHT in the absence or presence of Enz (10 µM) or vehicle (Ctrl) for 48 hours. mRNA expression of indicated lipid transporters

was analyzed by RNAseq, and heatmaps were generated with a hierarchical clustering algorithm using completed linkage and Euclidean distance measures and scaled by z score (red=positive z score, blue=negative z score). (C) mRNA expression of indicated lipid transporters was measured by qRT-PCR in LNCaP cells grown for 48 hours in CSS followed by treatment with 1 nM R1881 in the presence or absence of Enz (10 µM) for an additional 48 hours [n=3, mean±SD, One-way ANOVA with Dunnett's multiple comparisons test relative to vehicle (Ctrl ns=not significant, ****p<0.0001)]. (D) LNCaP cells were grown in CSS for 48 hours and treated with 10 nM DHT in the presence or absence of Enz (10 µM). Protein expression was measured by Western blot analysis and quantitated by densitometry analysis, and total protein levels were normalized to loading control (gamma tubulin) (mean±SD, One-way ANOVA with Dunnett's multiple comparisons test relative to vehicle control (CSS); a representative blot of three independent experiments is shown). (E) Cells were treated as described above. After fixation, cells were incubated with LDLR primary antibody for 24 hours and counterstained with appropriate secondary antibody. Protein expression was measured by qFM. (blue: DAPI, red: LDLR). (F) mRNA expression analysis of indicated lipid transporters and lipogenic genes in paired LNCaP tumor xenografts before (intact) and seven days after castration (nadir) of our previously reported longitudinal LNCaP tumor progression data set [34].

Figure 6: Androgen receptor regulates lipid uptake and lipogenesis. Schematic representation of cellular supply pathways of cholesterol and fatty acids in prostate cancer cells (transporter-mediated uptake, lipogenesis, passive diffusion, tunneling nanotubes). Lipid transporters and lipogenic enzymes whose expression is increased or decreased by androgens are highlighted in red and blue, respectively. Lipid transporters without confirmed surface expression in prostate cancer are marked by lighter shades of red and blue. Only lipid transporters with confirmed mRNA and protein expression in cell lines and patient samples are shown.

Fig1A

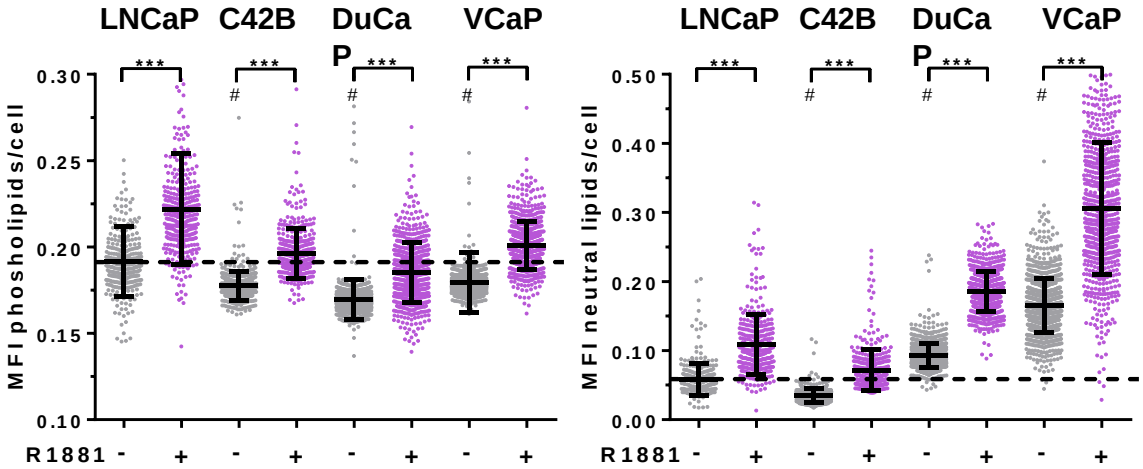

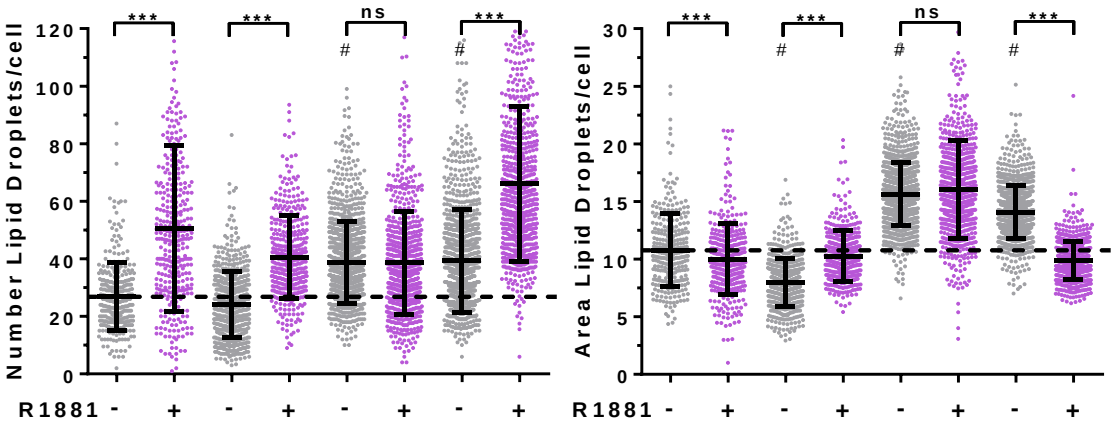

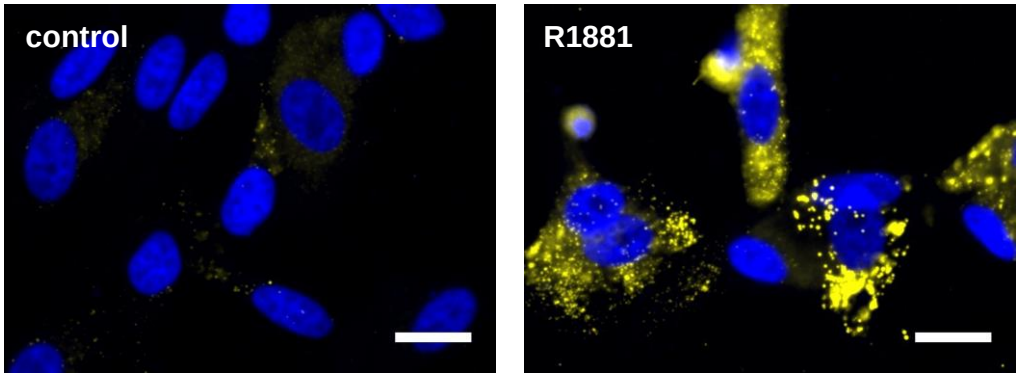

Fig2A

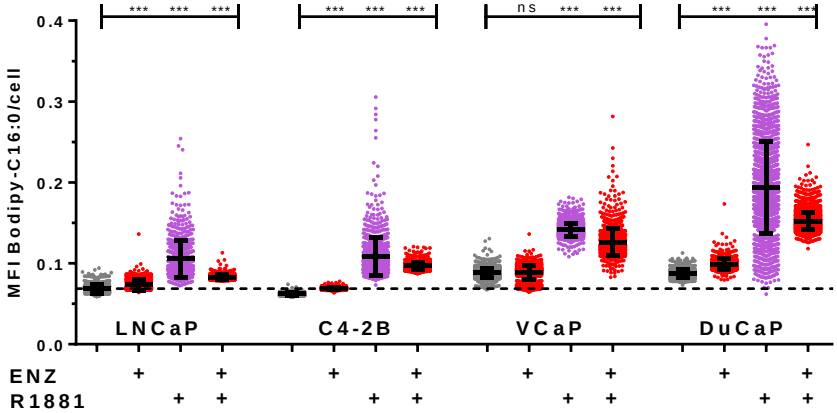

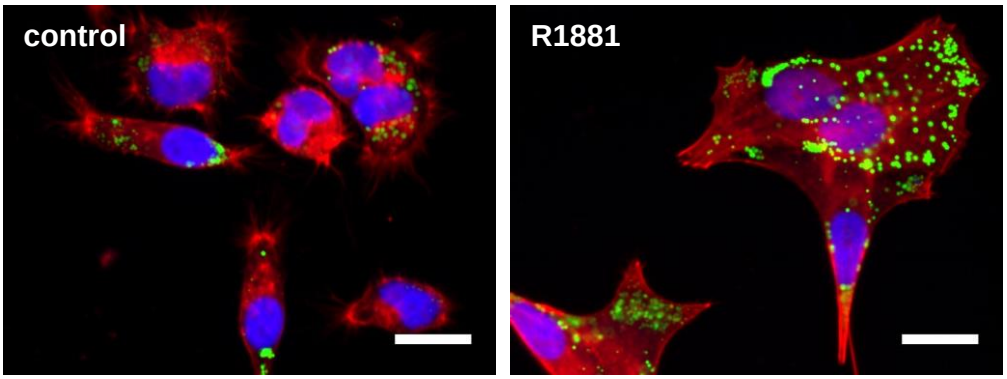

Fig2B

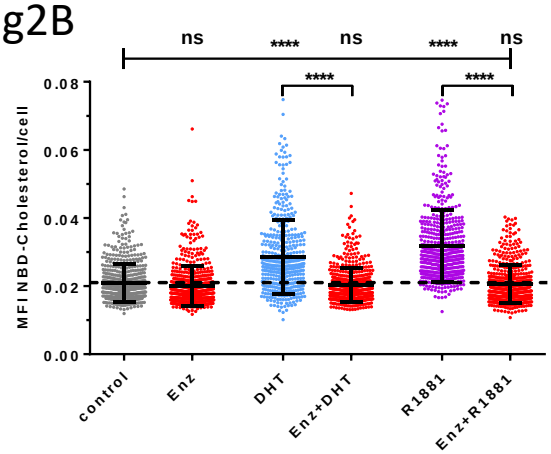

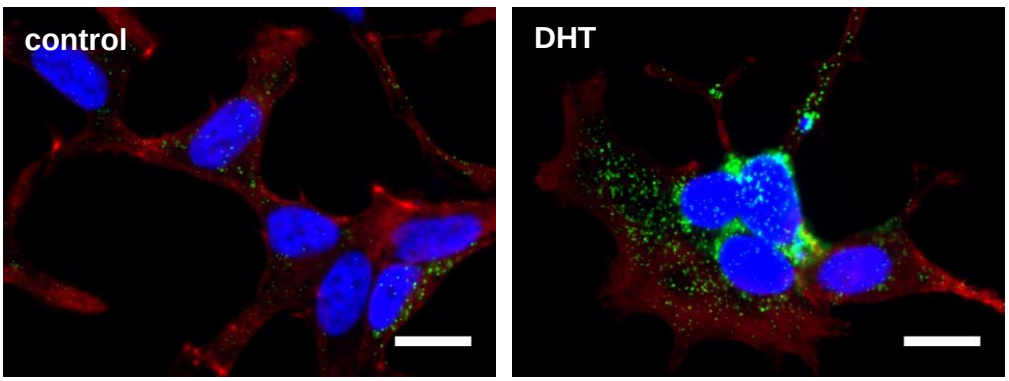

Fig2C

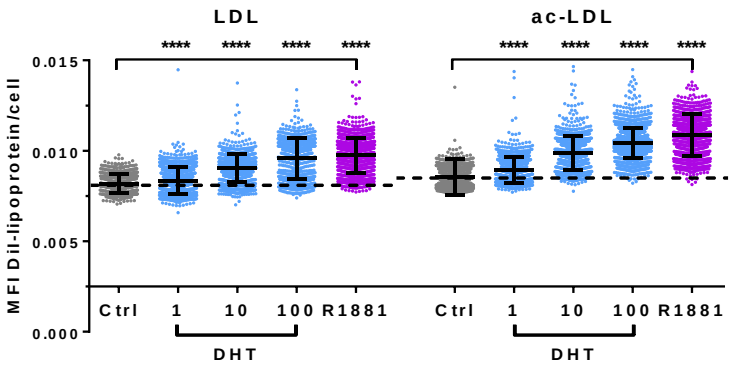

Fig3

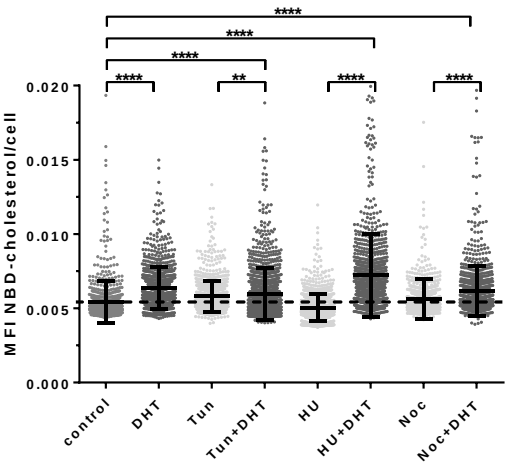

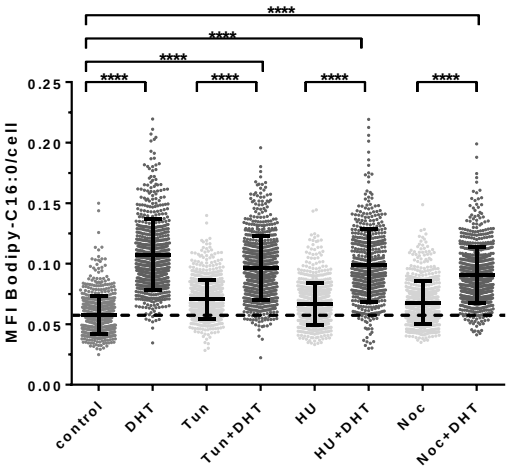

Fig4A

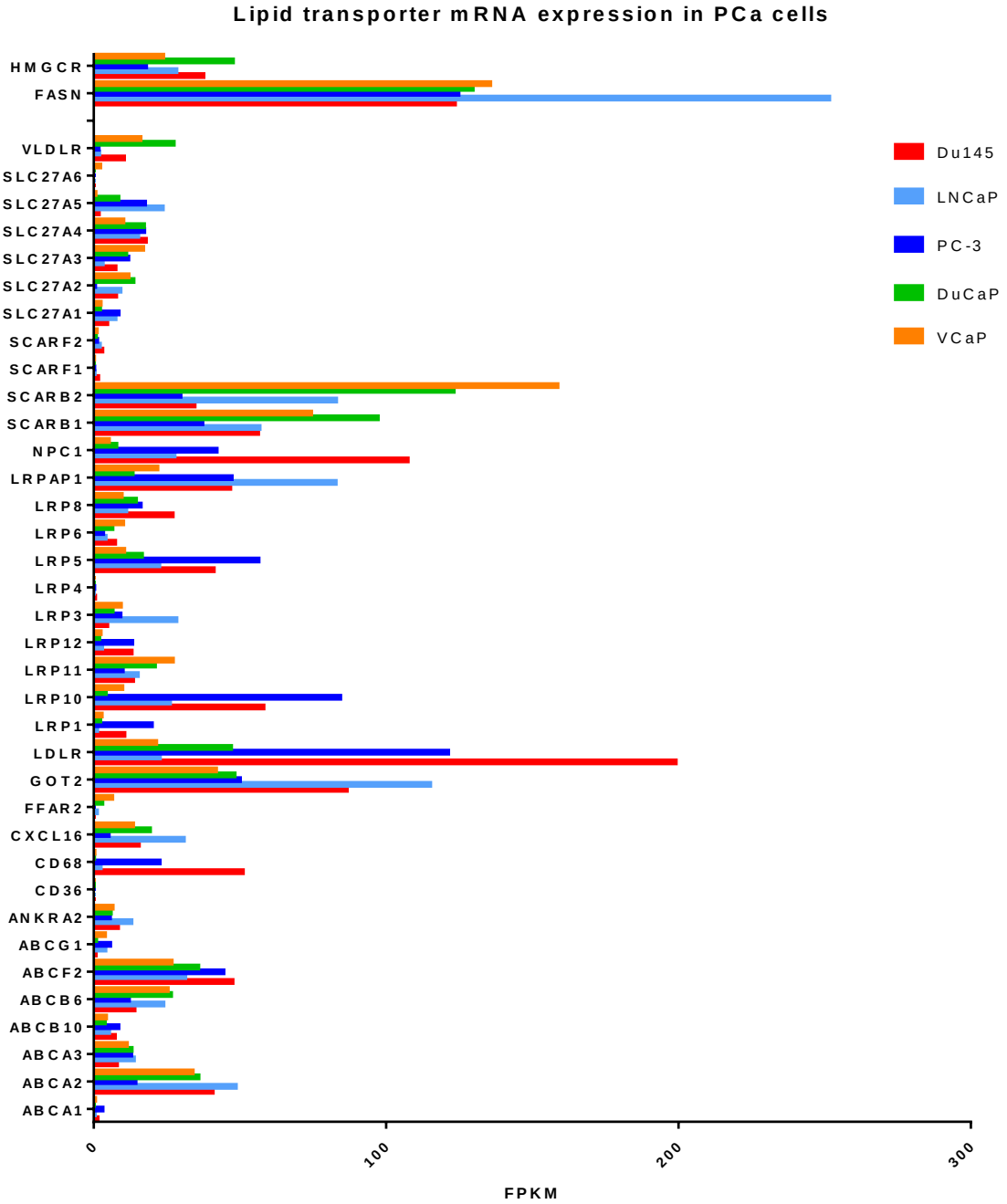

Fig4B

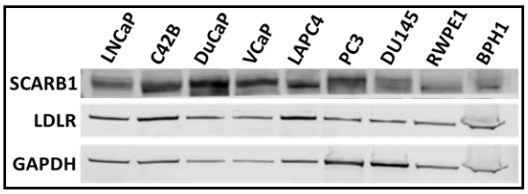

Fig4C

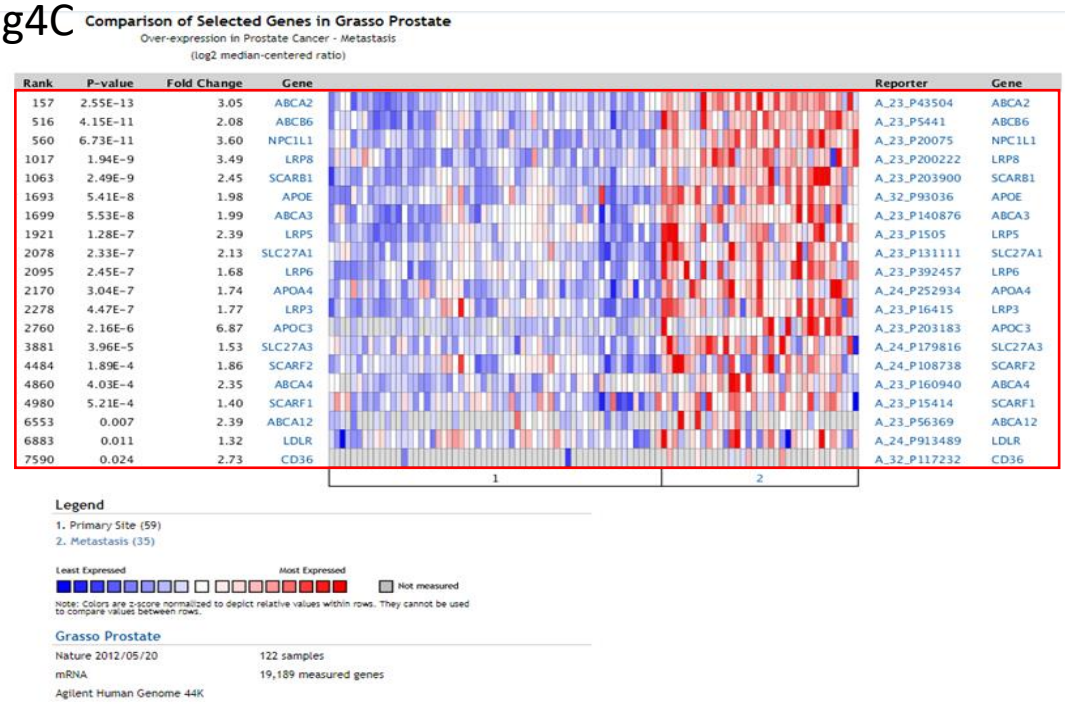

Fig4D

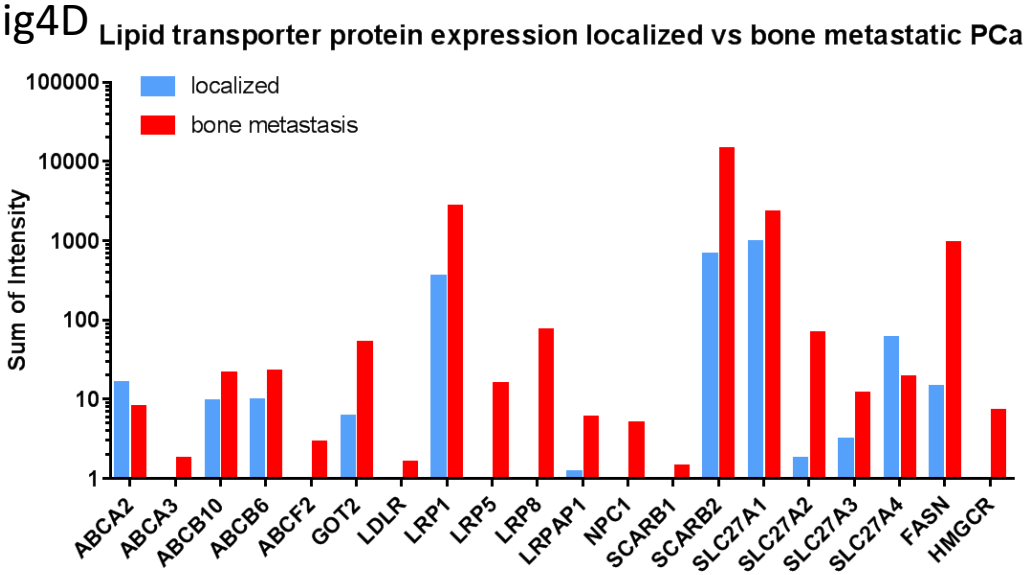

Fig4E

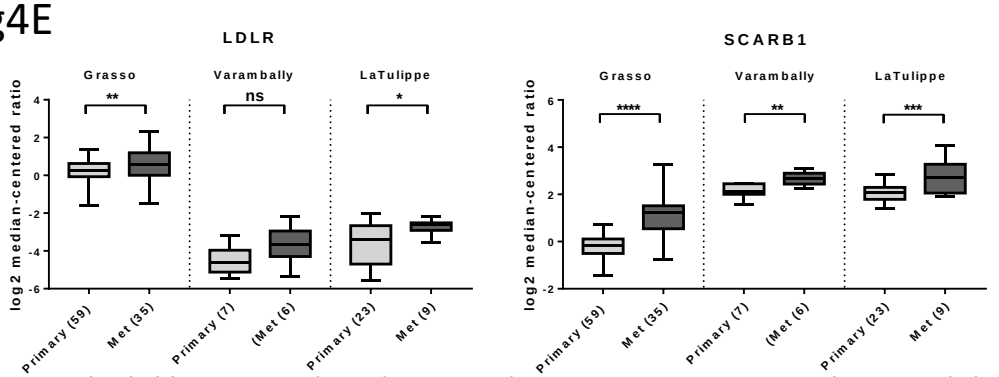

Fig5A

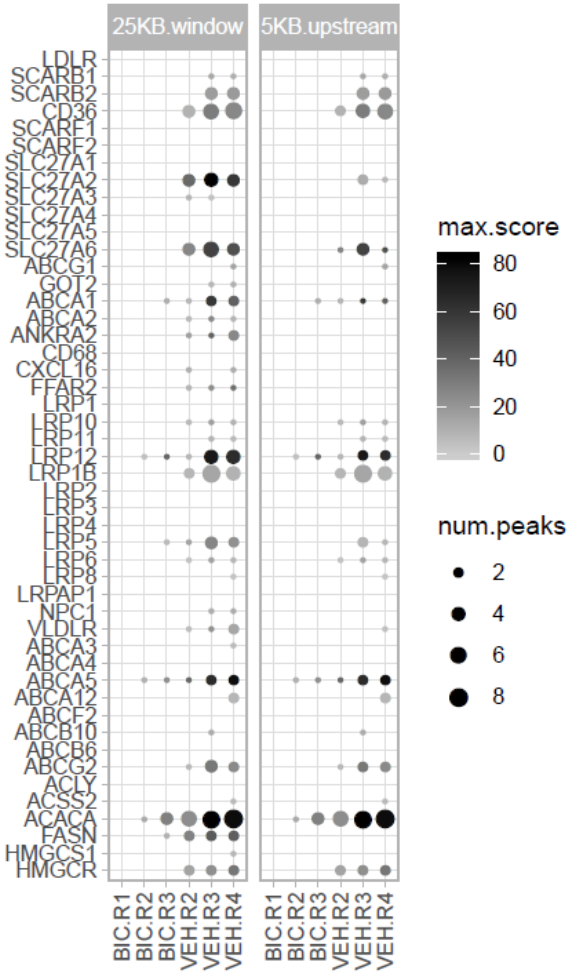

Fig5C

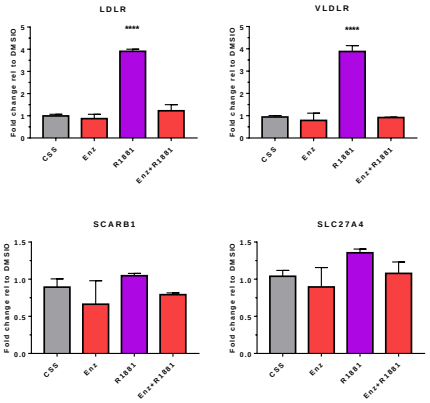

Fig5D

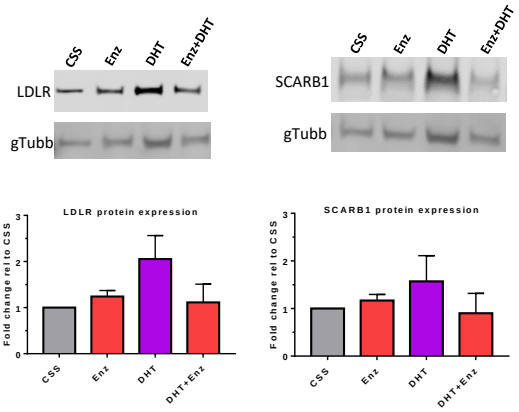

Fig5E

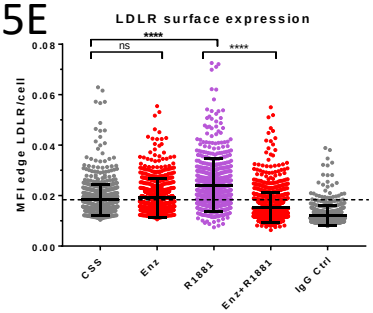

Fig5B

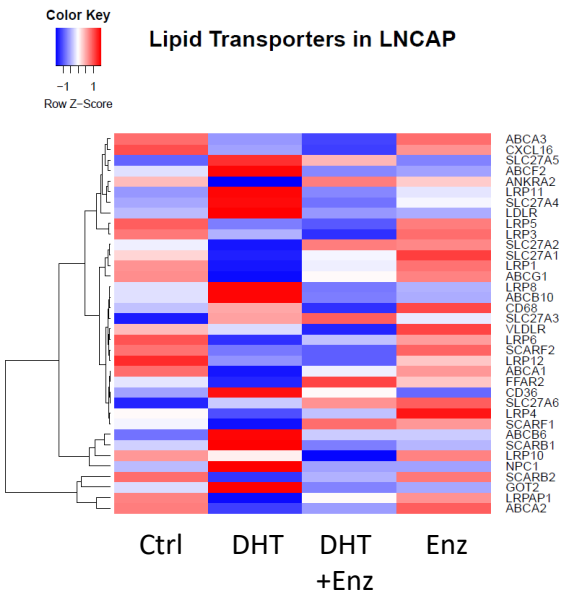

Fig5F

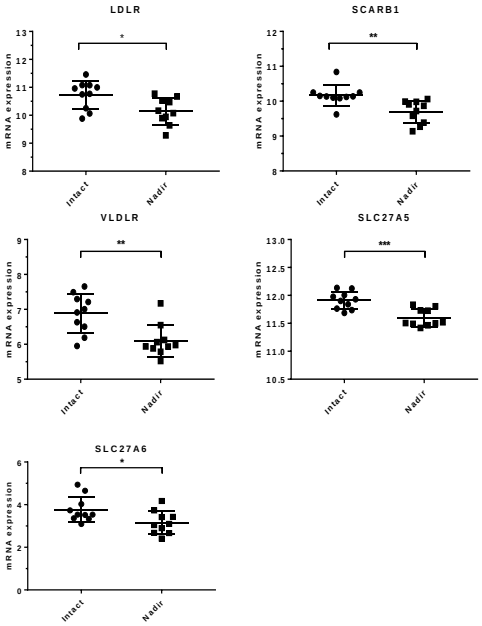

Fig6

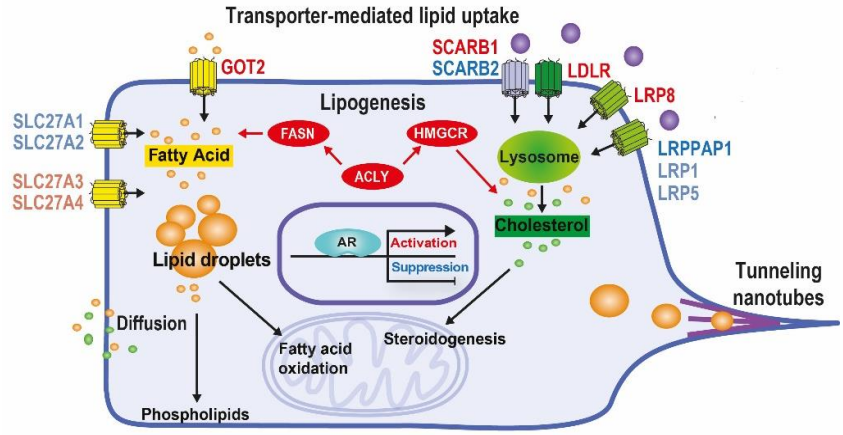

American Association for Cancer Research

Molecular Cancer Research

Lipid uptake is an androgen-enhanced lipid supply pathway associated with prostate cancer disease progression and bone metastasis

Kaylyn D Tousignant, Anja Rockstroh, Atefeh Taherian Fard, et al.

Mol Cancer Res Published OnlineFirst February 26, 2019.